



A reduced-order stochastic finite element analysis for structures with uncertainties

Ji Yang¹, Béatrice Faverjon^{1,2}, Herwig Peters¹, Nicole Kessissoglou¹

¹ School of Mechanical and Manufacturing Engineering, UNSW Australia, Sydney, NSW 2052, Australia

² Université de Lyon, CNRS, INSA-Lyon, LaMCoS UMR5259, F-69621, France

ABSTRACT

This work examines the effects of uncertain material and geometry properties on the dynamic characteristics of a simply supported plate. The forced responses of the plate are predicted using the polynomial chaos expansion method. The stochastic system equations are transformed to a set of deterministic equations using Galerkin projection. In order to improve the computational efficiency when attempting to examine the structure with many degrees of freedom, the Arnoldi-based Krylov subspace technique is implemented to reduce the number of degrees of freedom in the finite element model, before the polynomial chaos expansion is applied. The combined stochastic finite element analysis and model order reduction technique is shown to provide accurate results with significantly reduced computational effort.

Keywords: Polynomial chaos expansion, Model order reduction

1. INTRODUCTION

The uncertainties in geometry and material properties are generated during manufacturing or assembly process, which greatly affect the dynamic responses of engineering structures. Models of uncertainty are generally based on either a parametric or non-parametric description of uncertainty, or on a combination of both (1). In a parametric model of uncertainty, uncertain variables are statistically described using various techniques, such as the Monte Carlo simulation method (2), random factor method (3) and polynomial chaos expansion method (4). The Monte Carlo simulation can directly obtain the statistical characteristics of the outputs, which generates many samples of the uncertain variables to run simulations of the system. For accurate results, the sampling number in Monte Carlo simulation should be very large, which results in high computational cost. In the non-parametric models of uncertainty, the uncertainties can be described using a universal model and disregarding the details of uncertainties, such as the entropy optimization principle (5) and random matrix theory (6).

The polynomial chaos expansion (PCE) was first introduced as the homogeneous chaos (7). In the PCE method, the uncertain variables are represented by base polynomials. Using the orthogonality of the base polynomials, the stochastic system equations are transformed into a set of deterministic equations. Compared with Monte Carlo simulation, the PCE method can obtain the statistical characteristics of the results with greatly reduced computational cost. However, as the order of the PCE and the degrees of freedom of the dynamic system increase, the number of deterministic equations in the PCE simulation increases exponentially.

This paper examines the effects of uncertain Young's modulus and thickness on the frequency responses of a simply supported plate using polynomial chaos expansion. To further improve the computational efficiency, the polynomial chaos expansion method is combined with the Arnoldi-based Krylov subspace technique to reduce the model order. In this combined technique, only the order of the finite element model is reduced. The reduced order stochastic finite element technique is demonstrated to provide accurate results with significantly reduced computational effort. Based on the reduced order polynomial chaos expansion method, the effects of single and combined uncertainties are examined.

¹ ji.yang@unsw.edu.au

2. STOCHASTIC MODEL

Using polynomial chaos expansion method, the stochastic system equations are transformed into deterministic equations as follows. The uncertain variables are initially projected onto a stochastic space spanned by a set of mutually orthogonal base polynomials Ψ_i , which are functions of a multi-dimensional random variable $\boldsymbol{\xi} = \{\xi_1, \xi_2, \dots, \xi_n\}$. Every random variable has a corresponding random space $\xi_i \in \Omega_i$ ($i = 1, 2, \dots, n$). The uncertain variable χ can then be expressed as (8)

$$\chi = \sum_{i=0}^{\infty} x_i \Psi_i(\boldsymbol{\xi}) \quad (1)$$

where x_i are deterministic coefficients. The base polynomials Ψ_i are a set of multi-dimensional polynomials in terms of $\boldsymbol{\xi}$ with the following orthogonal relationship

$$E[\Psi_i, \Psi_j] = \delta_{ij} E[\Psi_i^2] \quad (2)$$

δ_{ij} is the Kronecker delta and E represents the expected value in the probability space. Selection of the base polynomials Ψ_i depends on the probability density function of each random variable (8).

Using the orthogonality relationship, the unknown coefficients x_i can be determined by stochastic Galerkin projection (8)

$$x_i = \frac{1}{E[\Psi_i^2]} \int_{\Omega} \chi \Psi_i(\boldsymbol{\xi}) d\mu(\boldsymbol{\xi}), \quad i = 0, 1, 2, \dots, \infty \quad (3)$$

$d\mu(\boldsymbol{\xi})$ is the probability measure in the random space Ω . If the random variables ξ_i are continuous and mutually independent, then $d\mu(\boldsymbol{\xi})$ can be expressed as

$$d\mu(\boldsymbol{\xi}) = \rho_1(\xi_1) \rho_2(\xi_2) \dots \rho_n(\xi_n) d\xi_1 d\xi_2 \dots d\xi_n \quad (4)$$

where $\rho(\xi)$ is the pdf of the random variable.

2.1 Frequency Response Analysis using Polynomial Chaos Expansion Method

The equation of motion for the dynamic system under external load is given by

$$(-\omega^2 \mathbf{M} + j\omega \mathbf{C} + \mathbf{K}) \mathbf{X} = \mathbf{F} \quad (5)$$

where \mathbf{M} is the mass matrix, \mathbf{C} is the damping matrix, \mathbf{K} is the stiffness matrix, ω is the excitation frequency, \mathbf{X} is the displacement vector, \mathbf{F} is the external force vector and $j = \sqrt{-1}$ is the imaginary unit. Assuming hysteretic damping yields

$$\mathbf{C} = \frac{\eta \mathbf{K}}{\omega} \quad (6)$$

where η is the damping loss factor. The equation of motion then becomes

$$(-\omega^2 \mathbf{M} + j\eta \mathbf{K} + \mathbf{K}) \mathbf{X} = \mathbf{F} \quad (7)$$

The uncertain stiffness matrix, mass matrix, force and displacement are represented using truncated PCE as

$$\mathbf{K}(\xi_K) = \sum_{p=0}^{N_K} \mathbf{K}_p \Psi_p(\xi_K), \quad \mathbf{M}(\xi_M) = \sum_{q=0}^{N_M} \mathbf{M}_q \Psi_q(\xi_M), \quad \mathbf{F}(\xi_F) = \sum_{u=0}^{N_F} \mathbf{F}_u \Psi_u(\xi_F), \quad \mathbf{X}(\boldsymbol{\xi}) = \sum_{s=0}^{N_X} \mathbf{X}_s \Psi_s(\boldsymbol{\xi}) \quad (8)$$

where N_K , N_M , N_F , N_X are respectively the number of polynomials to represent the stiffness and mass matrices, the force and displacement vectors.

Substituting the expansion equations given by Eq. (8) into Eq. (7), multiplying by a base polynomial $\Psi_t(\boldsymbol{\xi})$ and then using Galerkin projection results in

$$\begin{aligned}
& (1 + j\eta) \sum_{p=0}^{N_K} \sum_{s=0}^{N_X} \mathbf{K}_p \mathbf{X}_s E[\Psi_p(\xi_K) \Psi_s(\xi) \Psi_t(\xi)] - \omega^2 \sum_{q=0}^{N_M} \sum_{s=0}^{N_X} \mathbf{M}_q \mathbf{X}_s E[\Psi_q(\xi_M) \Psi_s(\xi) \Psi_t(\xi)] \\
& = \sum_{u=0}^{N_F} \mathbf{F}_u E[\Psi_u(\xi_F) \Psi_t(\xi)], \quad t = 0, 1, 2, \dots, N_t
\end{aligned} \tag{9}$$

where N_t is the number of base polynomials. For each excitation frequency ω , the deterministic coefficients of the polynomial chaos expansion for the displacement $[\mathbf{X}_0, \mathbf{X}_1, \dots, \mathbf{X}_N]^T$ are solved simultaneously.

2.2 Model Order Reduction

Model order reduction is implemented using the Arnoldi-based Krylov subspace technique to obtain a low-dimensional subspace with the transformation matrix $\mathbf{S} \in \mathcal{R}^{n \times m}$, which can approximate the original high-order vector \mathbf{Z} by the reduced-order vector \mathbf{Z}^r as follows (9,10)

$$\mathbf{Z} = \mathbf{S} \mathbf{Z}^r + \boldsymbol{\varepsilon} \tag{10}$$

$$\mathbf{S} \times \mathbf{S}^T = \mathbf{I}^n \tag{11}$$

$\mathbf{Z} \in \mathcal{R}^{n \times 1}$ and $\mathbf{Z}^r \in \mathcal{R}^{m \times 1}$ where $m \ll n$. $\mathbf{I}^n \in \mathcal{R}^{n \times n}$ is the identity matrix and m is the reduced number of degrees of freedom. The superscript r denotes the reduced-order matrix and $\boldsymbol{\varepsilon} \in \mathcal{R}^{n \times 1}$ is the negligible error. The transformation matrix \mathbf{S} is generated by the block Arnoldi algorithm (10).

Introducing Eqs. (10) and (11) into the stochastic system and projecting to the Krylov subspace yields

$$\begin{aligned}
& (1 + j\eta) \sum_{p=0}^{N_K} \sum_{s=0}^{N_X} \mathbf{K}_p^r \mathbf{X}_s^r E[\Psi_p(\xi_K) \Psi_s(\xi) \Psi_t(\xi)] - \omega^2 \sum_{q=0}^{N_M} \sum_{s=0}^{N_X} \mathbf{M}_q^r \mathbf{X}_s^r E[\Psi_q(\xi_M) \Psi_s(\xi) \Psi_t(\xi)] \\
& = \sum_{u=0}^{N_F} \mathbf{F}_u^r E[\Psi_u(\xi_F) \Psi_t(\xi)], \quad t = 0, 1, 2, \dots, N_t
\end{aligned} \tag{12}$$

where the reduced order mass matrix, stiffness matrix, displacement and force vectors are respectively defined as

$$\mathbf{M}^r = \mathbf{S}^T \mathbf{M} \mathbf{S}, \quad \mathbf{M} \in \mathcal{R}^{n \times n}, \quad \mathbf{M}^r \in \mathcal{R}^{m \times m} \tag{13}$$

$$\mathbf{K}^r = \mathbf{S}^T \mathbf{K} \mathbf{S}, \quad \mathbf{K} \in \mathcal{R}^{n \times n}, \quad \mathbf{K}^r \in \mathcal{R}^{m \times m} \tag{14}$$

$$\mathbf{X}^r = \mathbf{S}^T \mathbf{X}, \quad \mathbf{X} \in \mathcal{R}^{n \times 1}, \quad \mathbf{X}^r \in \mathcal{R}^{m \times 1} \tag{15}$$

$$\mathbf{F}^r = \mathbf{S}^T \mathbf{F}, \quad \mathbf{F} \in \mathcal{R}^{n \times 1}, \quad \mathbf{F}^r \in \mathcal{R}^{m \times 1} \tag{16}$$

3. NUMERICAL RESULTS

A rectangular simply supported plate of dimensions $L_x = 1350$ mm, $L_y = 1200$ mm and thickness $h = 5$ mm, with material properties of steel (density $\rho = 7800$ kg/m³, Young's modulus $E = 210$ GPa, Poisson's ratio $\nu = 0.3$) is examined. Damping is included using a complex Young's modulus $E(1 + j\eta)$ where $\eta = 0.03$ is the damping loss factor. The finite element model is developed in ANSYS using element type SHELL63. The plate is excited by a point force of unity amplitude located at $(0.6L_x, 0.6L_y)$. The mean and variance of the plate flexural velocity at a location of $(0.4L_x, 0.4L_y)$ on the plate are examined.

3.1 Uncertain Young's Modulus

Variability in the material properties is generated from an uncertain Young's modulus E , which is assumed to follow a lognormal distribution with mean $E[E] = 210$ GPa and variation coefficient $\delta_E = \frac{\sigma_E}{E[E]} = 5\%$, where σ_E is the standard deviation of Young's modulus E . The uncertain Young's

modulus is represented by the 3rd order Hermite PCE. The frequency responses are represented by the 5th order Hermite PCE. Results obtained using the PCE method are compared with Monte Carlo (MC) simulations using 5000 samples. Upper and lower envelopes of the frequency responses are constructed from the polynomial chaos expansion expression given by Eq. (1). In each case, 30,000 Hermite polynomial samples are generated and substituted into the PCE expression to obtain the maximum and minimum values of the plate flexural velocity. The original finite element model consists of 11,146 degrees of freedom. Considering a frequency range up to 100 Hz, the full model is reduced to an 80 degree-of-freedom system using the Arnoldi-based Krylov subspace technique.

The mean and variance of the frequency responses for $\delta_E = 2\%$ in the Young's modulus are presented in Fig. 1. The results in Fig. 1 from the reduced order PCE method and MC simulations are very close to each other. Compared with MC simulations, errors in the frequency response around the resonant peaks using polynomial chaos expansion are attributed to the level of uncertainty of the structural property as well as the location of adjacent peaks. The resonant peaks become broader with increasing frequency due to structural damping. As the frequency increases, the uncertainty has an increasing effect on the resonances with a decreasing effect on their magnitude.

The reduced order PCE method can obtain high accuracy with significantly reduced computational cost. For all simulations run on the same computer, the MC simulations take 48 hours and the reduced order PCE method takes 30 seconds. The significant improvement in computational cost using the model reduction technique is attributed to (i) the reduction in the degrees of freedom of the dynamic system from 11,146 to 80, thereby reducing the number of equations in the PCE analysis; (ii) the reduction in the size of the mass and stiffness matrices, which makes the matrix calculations faster.

Based on the reduced order polynomial chaos expansion methodology, the effects of different uncertain Young's modulus are examined. Figures 1(a)-1(c) present the mean and variance of the frequency responses as the level of uncertainty increases from $\delta_E = 2\%$ to $\delta_E = 5\%$ to $\delta_E = 10\%$, respectively. The frequency responses for uncertain Young's modulus are represented by the 5th order Hermite PCE. As the frequency and uncertainty level increase, the envelopes grow wider, showing increasing effects of uncertain Young's modulus.

3.2 Uncertain Plate Thickness

Variability in the geometric properties is examined by generating uncertainty in the plate thickness, which is assumed to follow a lognormal distribution with a mean value of $h = 5\text{mm}$. As the tolerance of thickness is generally very small, values for the variation coefficient of the plate thickness δ_h chosen here are also very small. In Figs. 2(a)-2(c), the variation coefficients of uncertainty in the plate thickness are 0.1%, 0.5% and 1% respectively. Uncertainty in the plate thickness is represented by the 2nd order Hermite PCE. The thickness parameter influences both the mass and stiffness matrices of the finite element model, involving h in the mass matrix and both h and h^3 in the stiffness matrix. The frequency responses for uncertain thickness are represented by the 6th order Hermite PCE. The frequency responses are influenced by the level of uncertainty in the plate thickness across the entire frequency range. The effects of uncertain thickness increase with frequency and the level of uncertainty. Compared with uncertain Young's modulus, the effect of uncertain thickness on the frequency responses is less significant for the variation coefficients values chosen here.

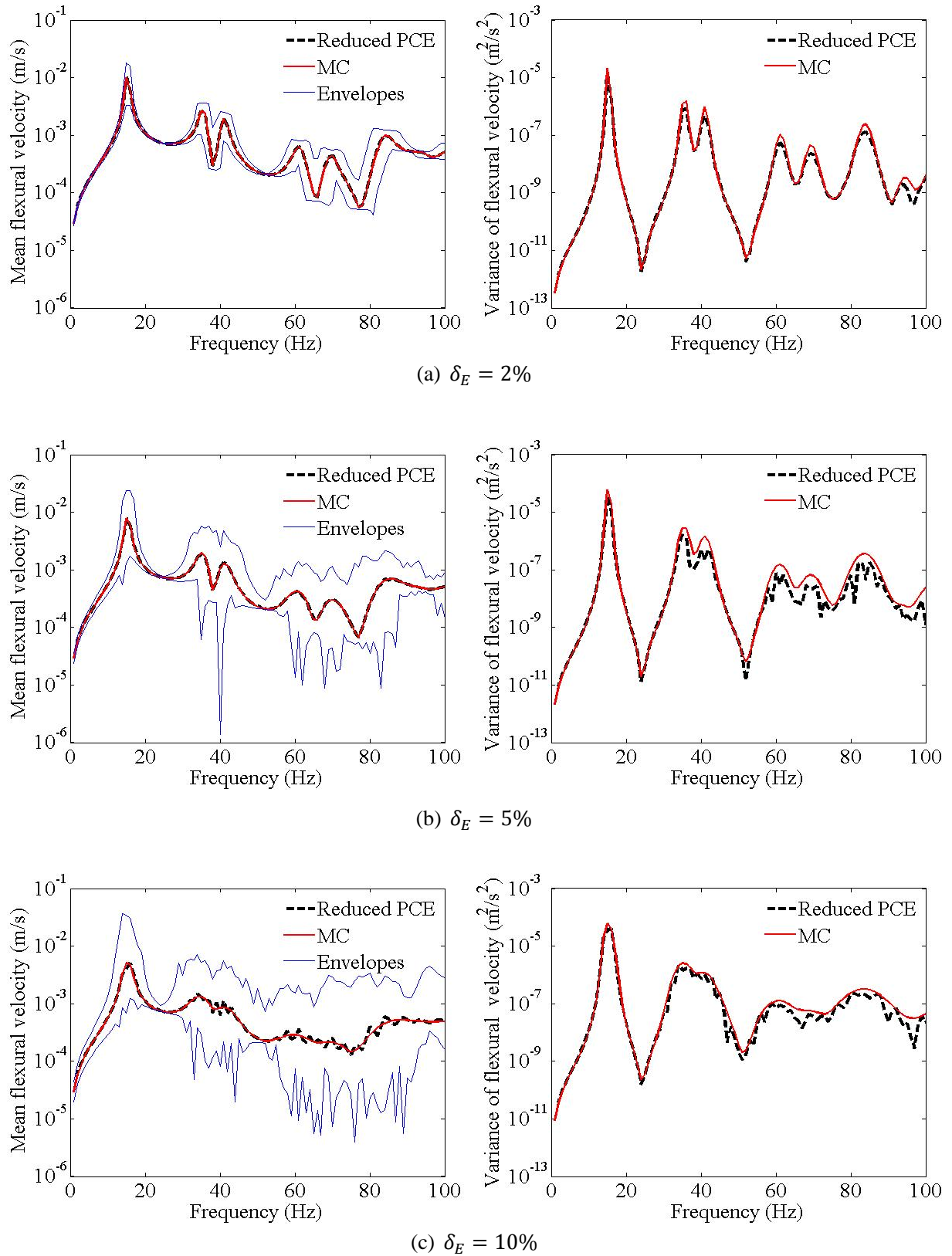


Figure 1 – Mean and variance of the frequency response using reduced PCE and Monte Carlo simulations for uncertain Young's modulus

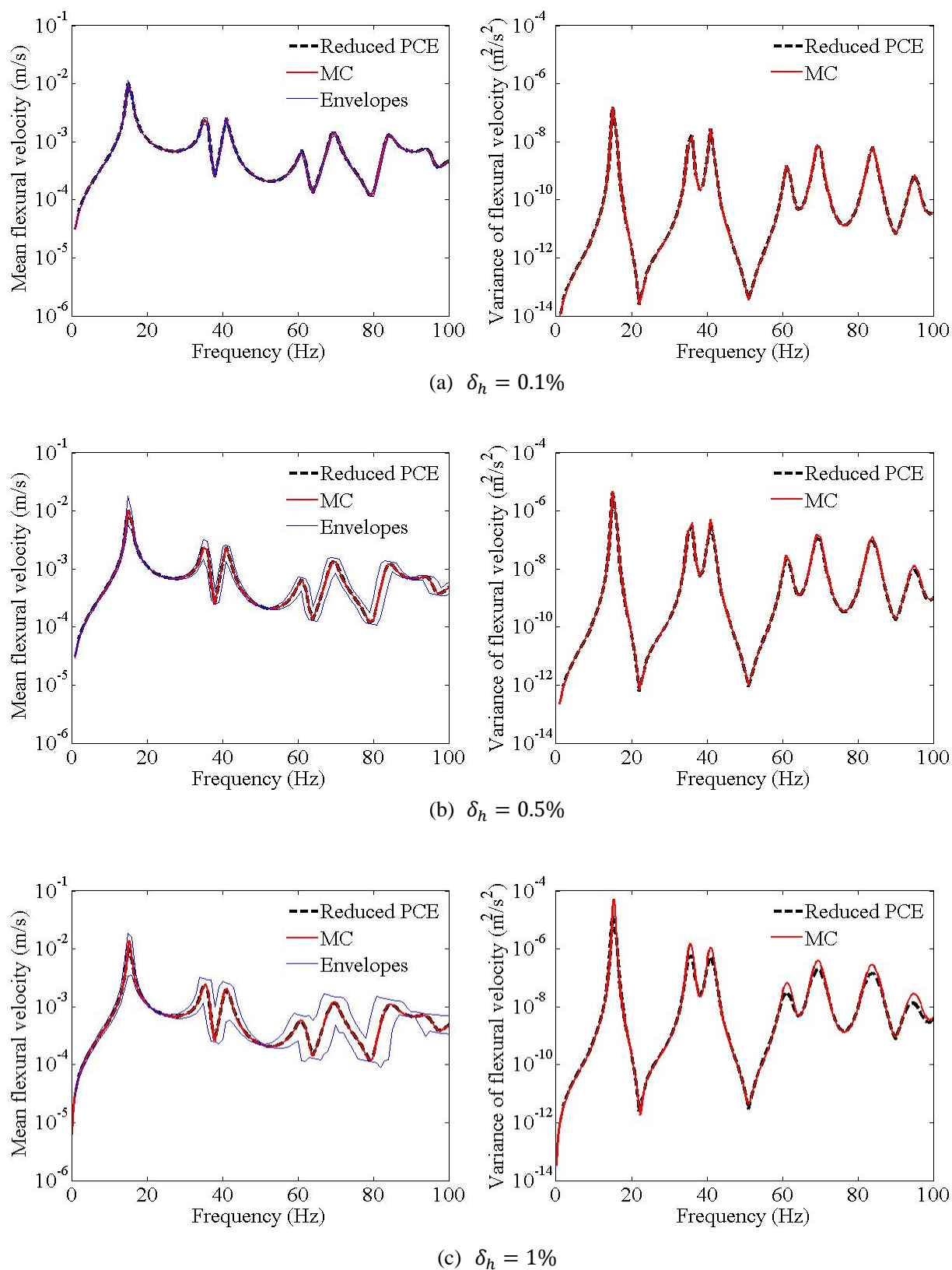


Figure 2 – Mean and variance of the frequency response using reduced PCE and Monte Carlo simulations for uncertain thickness

3.3 Uncertain Young's Modulus and Plate Thickness

To investigate the effect of combined uncertain parameters, the plate is now randomized by both Young's modulus and thickness as listed in Table 1. In each case, the frequency responses are represented by the 6th order 2-dimensional Hermite PCE. Figures 3 and 4 correspond to the frequency responses for cases 1 and 2 respectively, whereby the uncertain Young's modulus is kept fixed and the uncertain thickness increases. Comparing Figs. 3 and 4 shows that increasing the uncertain thickness only slightly affects the envelopes of the maximum and minimum responses around the resonant peaks. However, comparing Figs. 3 and 5 shows that increasing uncertainty in the Young's modulus affects the results across the entire frequency range. The effect of Young's modulus is dominant for the values of combined uncertainty examined here.

Table 1 – Combined uncertain parameters

Case	δ_E	δ_h
1	2%	0.1%
2	2%	0.5%
3	5%	0.1%

4. CONCLUSIONS

This paper examines a simply supported plate with uncertainties in its Young's modulus and thickness. The frequency responses of the plate flexural velocity are obtained, using the polynomial chaos expansion method. To further improve the computational efficiency, the Arnoldi-based Krylov subspace technique is combined with polynomial chaos expansion method to reduce the model order. Compared with Monte Carlo simulation, this combined stochastic technique is shown to work very well with significantly reduced computational cost. Both the uncertain Young's modulus and uncertain thickness are shown to affect the plate flexural responses across the entire frequency range. The effect of uncertain thickness is less significant for the values of uncertainty examined here.

ACKNOWLEDGEMENT

Béatrice Faverjon gratefully acknowledges the French Education Ministry, University of Lyon, CNRS, INSA of Lyon and LabEx iMUST for the CRCT and the out mobility grant.

REFERENCES

1. Ciciello A, Langley RS. The vibro-acoustic analysis of built-up systems using a hybrid method with parametric and non-parametric uncertainties. *J Sound Vib.* 2013; 332: 2165–2178.
2. Fishman GS. Monte Carlo: Concepts, Algorithms, and Applications. New York: Springer; 1995.
3. Gao W, Kessissoglou NJ. Dynamic response analysis of stochastic truss structures under non-stationary random excitation using the random factor method. *Comput Meth Appl Mech Eng.* 2007; 196: 2765-2773.
4. Ghanem RG, Spanos PD. Stochastic Finite Elements: A Spectral Approach. New York: Springer-Verlag; 1991.
5. Soize C. A comprehensive overview of a non-parametric probabilistic approach of model uncertainties for predictive models in structural dynamics. *J Sound Vib.* 2005; 288(3): 623-652.
6. Kessissoglou NJ, Lucas GI. Gaussian orthogonal ensemble spacing statistics and the statistical overlap factor applied to dynamic systems. *J Sound Vib.* 2009; 324: 1039-1066.
7. Wiener N. The homogeneous chaos. *Am J Math.* 1938; 60: 897-936.
8. Sepahvand K, Marburg S, Hardtke HJ. Uncertainty quantification in stochastic systems using polynomial chaos expansion. *Int J Appl Mech.* 2010; 2: 305-353.
9. Bai ZJ. Krylov subspace techniques for reduced-order modeling of large-scale dynamical systems. *Appl Numer Math.* 2002; 43(1-2): 9-44.
10. Han JS, Rudnyi EB, Korvink JG. Efficient optimization of transient dynamic problems in MEMS devices using model order reduction. *J Micromech Microeng.* 2005; 15(4): 822-832.
11. Sinou JJ, Faverjon B. The vibration signature of chordal cracks in a rotor system including uncertainties. *J Sound Vib.* 2012; 331(1): 138-154.

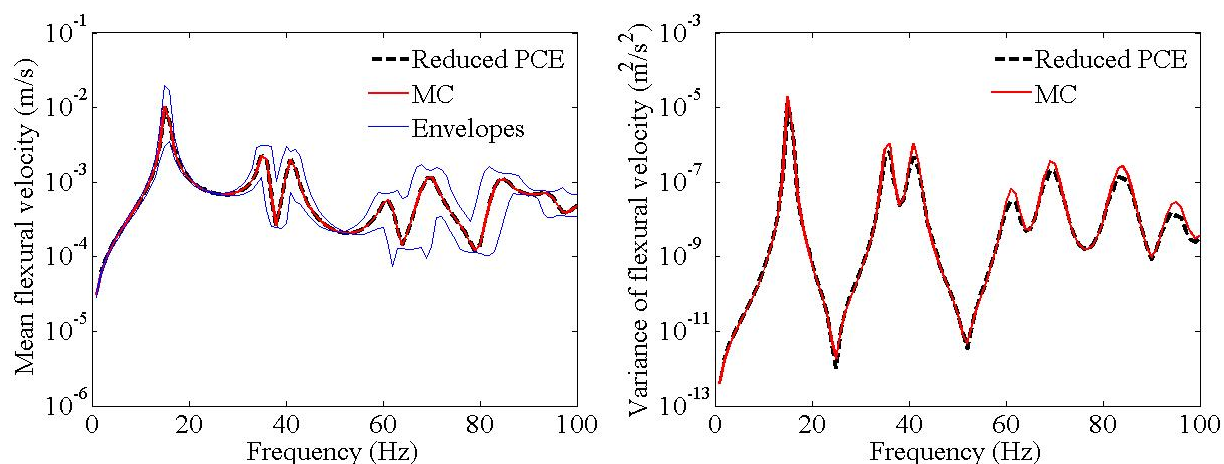


Figure 3. Mean and variance of the frequency response using reduced PCE and Monte Carlo simulations for two uncertain parameters ($\delta_E = 2\%$, $\delta_h = 0.1\%$)

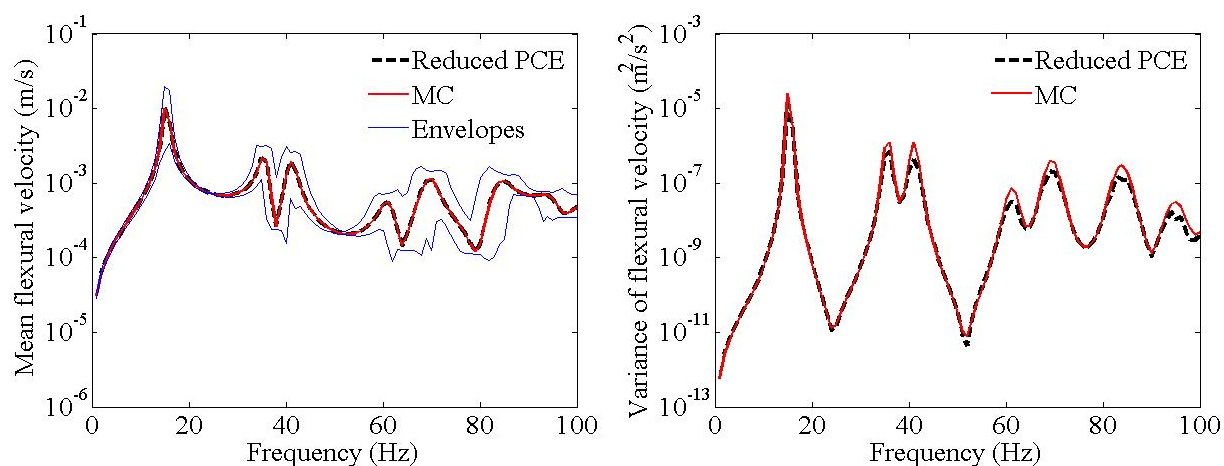


Figure 4. Mean and variance of the frequency response using reduced PCE and Monte Carlo simulations for two uncertain parameters ($\delta_E = 2\%$, $\delta_h = 0.5\%$)

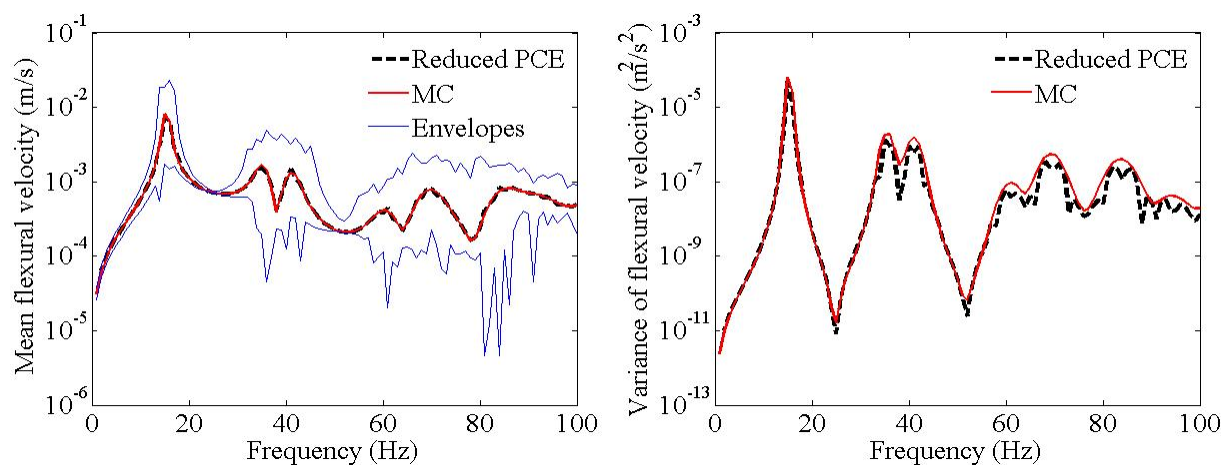


Figure 5. Mean and variance of the frequency response using reduced PCE and Monte Carlo simulations for two uncertain parameters ($\delta_E = 5\%$, $\delta_h = 0.1\%$)